

Calculation of Decomposition Products from Components of Gunpowder by using ReaxFF Reactive Force Field Molecular Dynamics and Thermodynamic Calculations of Equilibrium Composition

Tomas L. Jensen,^[a] John F. Moxnes,^{*[a]} Erik Unneberg,^[a] and Ove Dullum^[a]

Abstract: The major combustion products from munitions containing nitro-based propellants are water, carbon monoxide, carbon dioxide, hydrogen, and nitrogen. In addition, compounds including hydrogen cyanide, ammonia, methane, nitrogen oxides, benzene, acrylonitrile, toluene, furan, aromatic amines, benzopyrene, and various polycyclic aromatic hydrocarbons are detected in minor concentrations. The literature shows that the thermodynamic prediction of the major decomposition products agrees fairly well with the measurements. However, poor agreement is found for the minor species. We have studied the thermal decomposition products of the main gunpowder ingredients. Each of the components nitrocellulose, nitroglycerine, and the

nitrate ester stabilizers diphenylamine and ethyl centralite were thermally decomposed with ReaxFF reactive force field molecular dynamics and equilibrium thermodynamics. The molecular dynamics results for the major decomposition products from nitrocellulose were partly consistent with measurements. Compared to the thermodynamic calculations, the molecular dynamics simulations agreed considerably better with experimental results for minor species like hydrogen cyanide. The nitrate ester stabilizers are the main sources for ammonia and aromatic combustion products, whereas hydrogen cyanide is produced from nitrocellulose as well as from the stabilizers when gunpowder is combusted.

Keywords: Gunpowder · Molecular dynamics · Reactive force field · Combustion products

1 Introduction

Decomposition products from firing weapons with conventional nitro-based propellants are highly complex mixtures of gases, vapors, and particles. In addition to the major oxidation products (H_2O , CO , CO_2 , H_2 , and N_2) low levels of numerous compounds including HCN, NH_3 , CH_4 , nitrogen oxides, benzene, acrylonitrile, toluene, furan, aromatic amines, benzopyrene, and other polycyclic aromatic hydrocarbons have been identified in emission from M16 rifle using nitro-based propellant [1]. Indeed, many of the identified chemical species have known toxicological issues, and even mutagenic effects [2,3]. It has been suggested that aromatic and/or nitroaromatic amines are responsible for the mutagenic activity [2]. In a similar manner as potent aromatic hydrocarbons are formed from diesel exhaust, it has been suggested that propellant ingredients like nitrocellulose, nitroglycerine, centralite I, diphenylamine, potassium nitrate, phthalates and graphite may produce nitroaromatic amines in the open-air burning, whereas aromatic amines are generated in the reducible atmosphere of the guns [4]. Volk et al. measured the reaction products from a double base propellant and found that the formation of HCN was dependent on the pressure. At high pressure, no

HCN was measured, while at low pressure a significantly amount of HCN was detected [5].

Pyrolysis has been used to study the decomposition products from energetic materials such as nitrocellulose and nitroglycerine [6,7]. Cropek et al. performed qualitative pyrolysis experiments of the individual components that are common in gunpowder [8]. These experiments show that nearly all the incompletely decomposed products are remnants of additives and not from the main energetic components in gunpowder. Benzene, phenol, and nitroaromatic compounds are typically the incomplete decomposition products from the stabilizer 2-nitrodiphenylamine.

The major combustion products of most propellants are classified as (a) tissue asphyxiants (CO , NO , and HCN), (b) irritant gases such as NH_3 , NO_2 , NO , SO_2 , HCl, and (c) inhaled metal particles such as lead, copper, and zinc, which main source may be the projectile, and to some extent the

[a] T. L. Jensen, J. F. Moxnes, E. Unneberg, O. Dullum
Norwegian Defence Research Establishment (FFI)
P.O. Box 25
2027 Kjeller, Norway
*e-mail: john-f.moxnes@ffi.no

primer and the propellant. The absorption of gases depends mainly on their solubility in the aqueous layer lining the mucosa in the upper and lower respiratory tracts. HCN leads to cellular asphyxia by interfering with the cell's cytochrome oxidase system. Due to its high water solubility, ammonia is an upper respiratory tract, eye, and skin irritant [9].

Due to the conditions of very high temperature and pressure it is a challenge to understand the decomposition and subsequent reactions of high-explosive materials in in-bore propellants decomposition. Several computer models are available to predict the composition of combustion products at steady state conditions (thermodynamic equilibrium). The prediction of the major chemical species agrees fairly well with the measurements. The concept of frozen equilibrium appears to apply only for N_2 , H_2 , CO , and CO_2 (at around 1500–1800 K) [10,11]. However, there is a rather poor agreement for the minor species, which are produced during decomposition, especially the organic compounds. It has been shown that the experimental results for NH_3 and HCN are several orders of magnitude higher than their thermodynamically calculated concentrations [11]. Overall, the theoretical concentrations of trace species based on thermodynamic equilibrium in combustion appear to be less important.

Molecular dynamics (MD) can be used to study situations different from steady-state conditions. The fundamental input in MD simulations is the atomic interactions, which are described from first principles by quantum mechanics (QM). One computational approach is to perform a number of density functional theory (DFT) calculations to compute interatomic forces quantum mechanically, in parallel with a classical calculation of the position time history of the atoms. MD is capable of revealing changes in the atomic and electronic structures that may not be captured by steady-state calculations [12–15]. Unfortunately, DFT based MD methods are so far computationally too demanding to describe most processes, where chemical reactions are involved. Studies have been most useful for understanding unimolecular and simple bimolecular processes of small molecules. It is notable that classical force fields can be used to describe the energy, structures, and vibrations of molecular systems. However, classical force fields cannot be applied to calculate chemical reactions, thus limiting the method's range of applicability.

The limitation of DFT based MD and classical force fields has to some extent been overcome by the development of reactive force field molecular dynamics (ReaxFF-MD), which is able to describe chemical reactions in a computationally efficient way [16–23]. The ReaxFF-MD concept was introduced by Tersoff in 1988 [24]. Using the concept of partial bond order as base the ReaxFF-MD enables MD simulations at computational costs nearly as low as those for classical force fields. A fundamental difference between the ReaxFF-MD and unreactive force fields is that ReaxFF-MD does not assume a fixed connectivity assignment for the chemical

bonds. Instead, the bond order is calculated from the interatomic distances which are changing continuously during the dynamics. [The energy of the system is described as the sum of various energy distributions. It can be divided into three parts: (a) covalent interactions (bonds, angles, and torsion) based on the concept of bond order, (b) coulomb forces between all atom pairs, (c) van der Waals forces between all pairs of atoms.]. This allows for the creation and dissociation of bonds during a simulation. The parameters of the inter-atomic potentials are "trained" to best-fit thousands of DFT calculations on small clusters of various atomic species combinations.

The parameters of the nitramines are, for instance, based on a large number of *ab initio* QM calculations. More than 40 reactions and 1600 molecules have been used. The major problem is whether the potential energy expression in ReaxFF-MD can produce reasonable dynamics on systems outside its training set. ReaxFF-MD is now in practical use for studying high-temperature and high pressure MD of realistic and chemically reacting systems. It has been applied to describe the thermal decomposition of RDX [21,25], TATP [18], PETN [26], TATB, and HMX [22]. ReaxFF-MD predicts that by 30 ps (pico seconds) TATB decomposition initiates the formation of large carbon clusters, whereas HMX decomposition leads almost directly to small-molecule products. This is in full agreement with experimental observations and demonstrates that ReaxFF-MD is a viable method. Diao et al. [27] used the same force field to simulate thermal decomposition of epoxy resins, which is a non-energetic molecular system.

The objective of this study was to quantitatively determine the thermal decomposition products of the components in gunpowder. Nitrocellulose, nitroglycerin, diphenylamine, and ethyl centralite were separately thermally decomposed in molecular dynamics simulations. The results are compared with thermodynamic calculations and pyrolysis experiments. Particular emphasis is placed on toxic species like HCN, NH_3 and aromatic hydrocarbons, but other common decomposition products are also studied. Section two presents the basis for the theoretical calculations and the pyrolysis experiments. The results from the calculations and experiments are discussed in Section three and Section four concludes.

2 Computational Details

Molecular dynamics simulations were performed with the ADF ReaxFF version 2010.02 software [17]. The two main ingredients in double base gunpowder, nitroglycerine (NG) and nitrocellulose (NC), and two common nitrate ester stabilizers, diphenylamine (DPA) and ethyl centralite (EC), were thermally decomposed using the ReaxFF-MD. We created a model molecule of NC (14.0% N) consisting of five repeating units (Figure 1). The molecule chain is terminated with an OH group at each end. Model molecules of NC

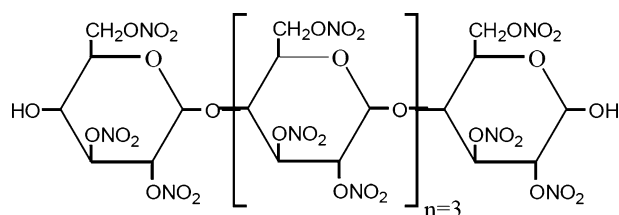


Figure 1. The NC model molecule (14.0% N).

with 12.9% N and 11.6% N are also used in the simulations. These molecules have two and four ONO_2 groups, respectively, substituted with OH. The NG, NC, DPA, and EC molecule structures were optimized by using the Gaussian09 software with the semi-empirical method PM6 [28].

The simulations were performed at three temperatures (2000 K, 3000 K, and 4000 K) and four states (1–4) with the densities of 1140 kg m^{-3} , 292 kg m^{-3} , 59 kg m^{-3} , and 2.6 kg m^{-3} in order to study how temperature and density influence the formation of decomposition products. These densities correspond to the density in the solid phase, the peak gas density in the gun barrel (chamber pressure), the density when the bullet leaves the barrel and finally, the density at atmospheric pressure.

The optimized structure of 43 DPA molecules was placed in a $3.5 \text{ nm} \times 3.5 \text{ nm} \times 3.5 \text{ nm}$ box in ReaxFF-MD. This corresponds to a density of 292 kg m^{-3} , equivalent to the chamber pressure in the gun. In order to simulate the thermal decomposition, we performed an energy minimizing of the system at 0 K. The temperature of the system is increased from 0 K to the target temperature. The heating rate was 2 K per fs and the system was simulated for 250 ps. The ReaxFF-MD NVT simulations applied the Velocity Verlet method with the Berendsen thermostat and a damping constant of 100 fs for temperature control. The same procedure and simulations were performed for NG, NC and EC. For NG and EC, there were 33 and 28 molecules in the box,

respectively, whereas 25 units (i.e. five model molecules) were used for NC. The numbers of molecules in the boxes were kept constant, while the volumes of the boxes were changed according to the different densities. For the thermodynamic calculations, we used the CEA code [29].

Pyrolysis experiments were carried out by heating 0.2 g sample with two gas burners in an argon-filled reaction bottle. A condenser was connected to the bottle. The decomposition products were transferred by an argon gas flow of 100 mL min^{-1} from the reaction bottle and into a 55-liter container to dilute the sample. A Gasetm DX4000 FTIR was used for quantitative analyses of the decomposition products (CO , N_2O , NO , NO_2 , NH_3 , CH_4 , HCN , H_2O) in the gas tank. In the pyrolysis experiments, DPA and EC were used as received from Sigma-Aldrich.

3 Results and Discussion

3.1 Steady State Results (Thermodynamic Equilibrium)

Table 1 shows the gunpowder composition. Moxnes et al. [11] show that measured values are 1–2 orders of magnitude larger than the equilibrium concentrations for HCN and NH_3 in state 3, and many orders of magnitude higher if we compare with the theoretical results in open space (state 4).

Without the two stabilizers the amount of HCN is significantly lower, see Figure 2. In state 4, the thermodynamic

Table 1. Gunpowder composition.

Ingredients	Powder 1/mass%
Nitrocellulose	74–77
Nitroglycerine	13–16
Diphenylamine	1.2
Ethyl centralite	5.5

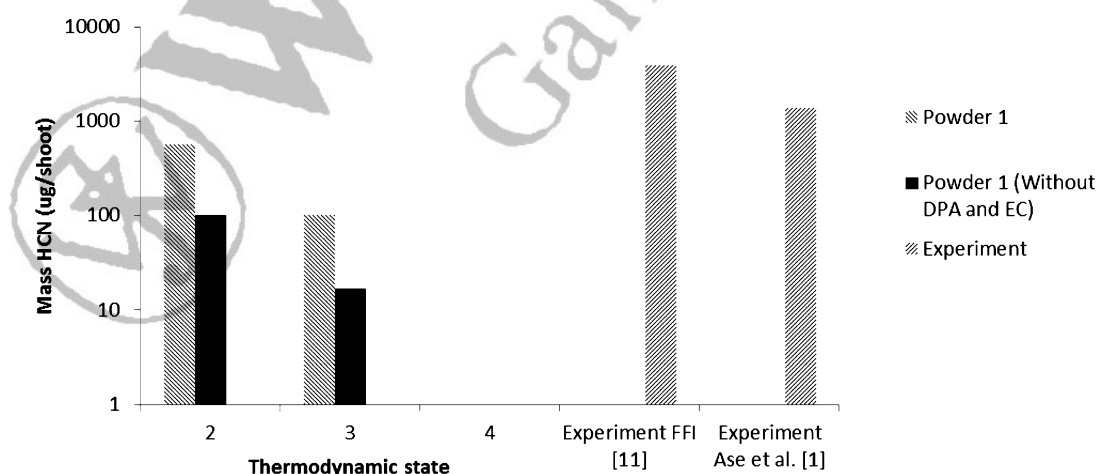


Figure 2. Calculated equilibrium concentration of HCN during a gunshot in state 2, 3, and 4, compared with experimental results. The temperature and density in state 2 are 3000 K and 292 kg m^{-3} , in state 3, 1830 K and 59 kg m^{-3} , and in state 4, 298 K and 2.6 kg m^{-3} , respectively.

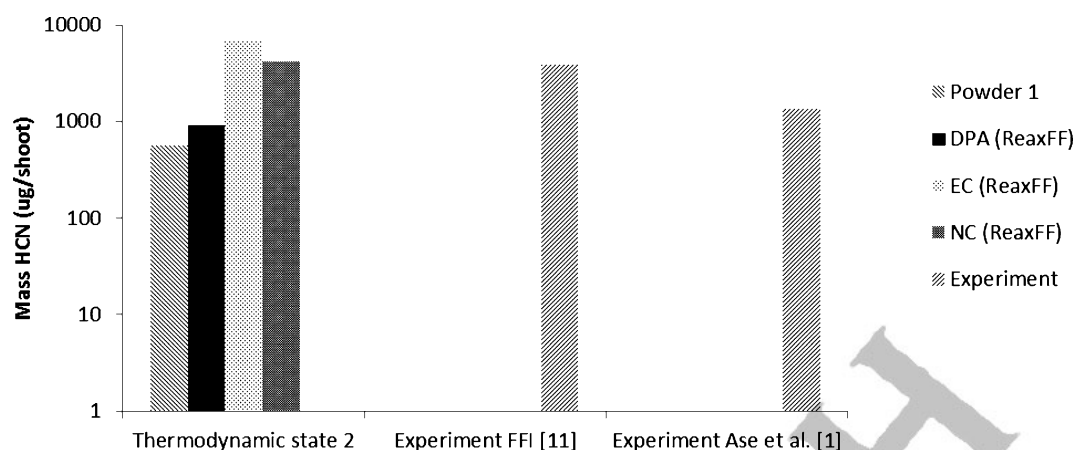


Figure 3. Mass of HCN per gunshot in state 2. Thermodynamic calculation, ReaxFF-MD simulation, and experimental results are compared. The temperature and density in state 2 are 3000 K and 292 kg m^{-3} .

analysis gives insignificant amounts of HCN. In the gun barrel, the temperature varies from 1800 K to 3000 K. The concept of frozen equilibrium appears to apply only for N_2 , H_2 , CO , and CO_2 (freezing temperature 1500–1800 K) [10, 11]. For HCN, however, the experimental measured concentration is higher than any calculated equilibrium concentration in the gun barrel. The concept of frozen equilibrium does not apply at any temperature (below 3000 K). To study this difference, we applied the ReaxFF-MD.

3.2 ReaxFF-MD and Thermodynamic Results

By using ReaxFF-MD we separately decomposed NC, NG, DPA, and EC thermally. It is seen from Figure 3 that NC, DPA and EC generate HCN during the decomposition process. The weight proportions of NC, DPA and EC are equivalent to the proportions in the gunpowder. Due to NG molecular structure and oxygen balance, insignificant amounts of HCN were formed in the thermal decomposition simulation of NG (data not shown). This result is in agreement with pyrolysis experiments [7].

If we add the amount of HCN generated from the separate decompositions by using ReaxFF-MD, we end up with around twice as much HCN as measured in experiments. The thermodynamic analysis gives a value seven times lower than measured, even if we use a freezing temperature of 3000 K. Thus, the ReaxFF-MD results do not match the thermodynamic results. Naturally, the comparisons have some limited validity since the gun powder ingredients are decomposed separately. We could not use ReaxFF-MD to simulate the thermal decomposition of the gunpowder with all four ingredients simultaneously because of computational capacity. However, separate ReaxFF-MD calculations give information about which substances may be the main sources of HCN and other toxic compounds in gunpowder.

We have studied how the number of molecules, simulation time, temperature, and density will affect the amount

of HCN and of the other main decomposition products. The number of HCN molecules generated during the decomposition depends somewhat on the number of NC molecules in the starting configuration (Figure 4). It is formed between 0.06 and 0.12 HCN molecules per unit NC. Changing the initial number of molecule for NG, DPA, and EC has only minor influence on the simulation results.

The degree of nitration of NC may vary. The amount of HCN formed when NC decomposes will depend upon the degree of nitration (Figure 5).

Figure 6 shows the major decomposition products from NC. After about 100 ps, the number of the decomposition products is relatively stable, showing that a simulation time of 250 ps will be sufficient.

In Figure 7 the thermal decomposition products from NC are compared with experimental data. The experimental data were obtained from pyrolysis carried out at atmospheric pressure [6]. At a density of 292 kg m^{-3} , the simulated amounts of CO and CO_2 are fairly in agreement with experimental data. There is also partial agreement with NO , while the agreement is relatively poor for CH_2O , H_2O , and HCN. Thermodynamic equilibrium calculation agrees well for CO and CO_2 when compared against experimental data. However, these calculations predict negligible concentrations of HCN, CH_2O , NO , and NO_2 at 3000 K.

The ReaxFF-MD simulation of decomposition of NG is not as good as for NC, except for the amount of NO (Figure 8).

Decomposition of the nitrate esters starts in the solid or liquid phase and continues further in the gas phase. In these simulations, the initial configurations are chosen so that the entire decomposition process occurs in the gas phase. It was also attempted to calculate the NC and NG thermal decomposition in the solid phase. However, it was not possible to find a stable initial configuration. The system reacted even at the temperature 0 K. We used Packmol, which is an application in the ReaxFF software to find a starting position for the molecules [30]. In reference [26]

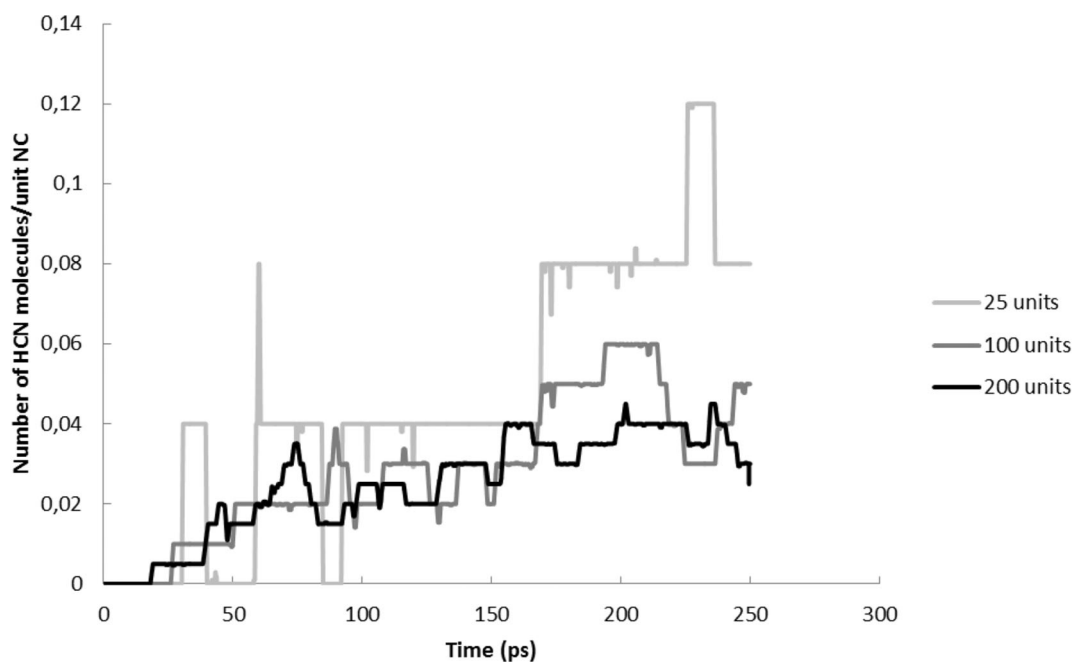


Figure 4. The number of HCN molecules per NC unit for different number of NC units in the starting configuration. The density (292 kg m^{-3}) and temperature (3000 K) correspond to state 2.

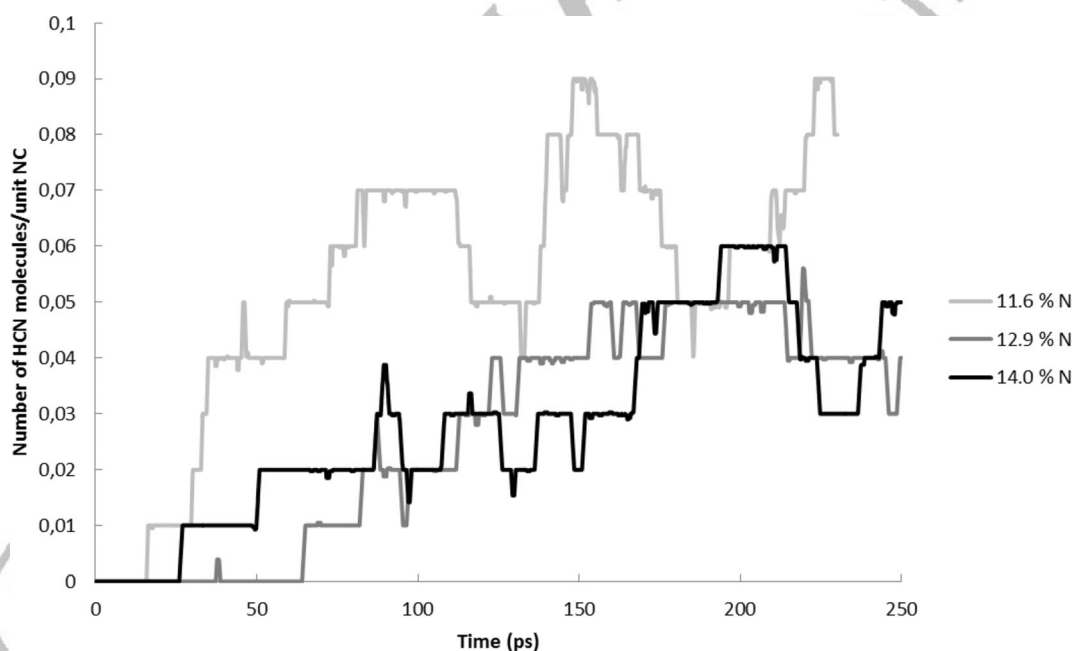


Figure 5. The number of HCN per NC unit for various nitration levels of NC. The temperature and density in state 2 are 3000 K and 292 kg m^{-3} , respectively. 100-NC units were used in the simulation.

the crystal structure for PETN was used as the starting configuration for ReaxFF simulations. Therefore, we may need to apply the exact crystal structure of NC and NG in order to find a stable initial configuration in the solid phase.

Figure 9 shows the formation of HCN from the decomposition of DPA for different temperatures. At 2000 K, 250 ps

is a too short simulation time since the level of HCN is rising and not being at steady state. The dotted lines in Figure 9 are thermodynamic equilibrium calculations at 3000 K and 4000 K. These results are consistent with ReaxFF-MD results at the same temperatures.

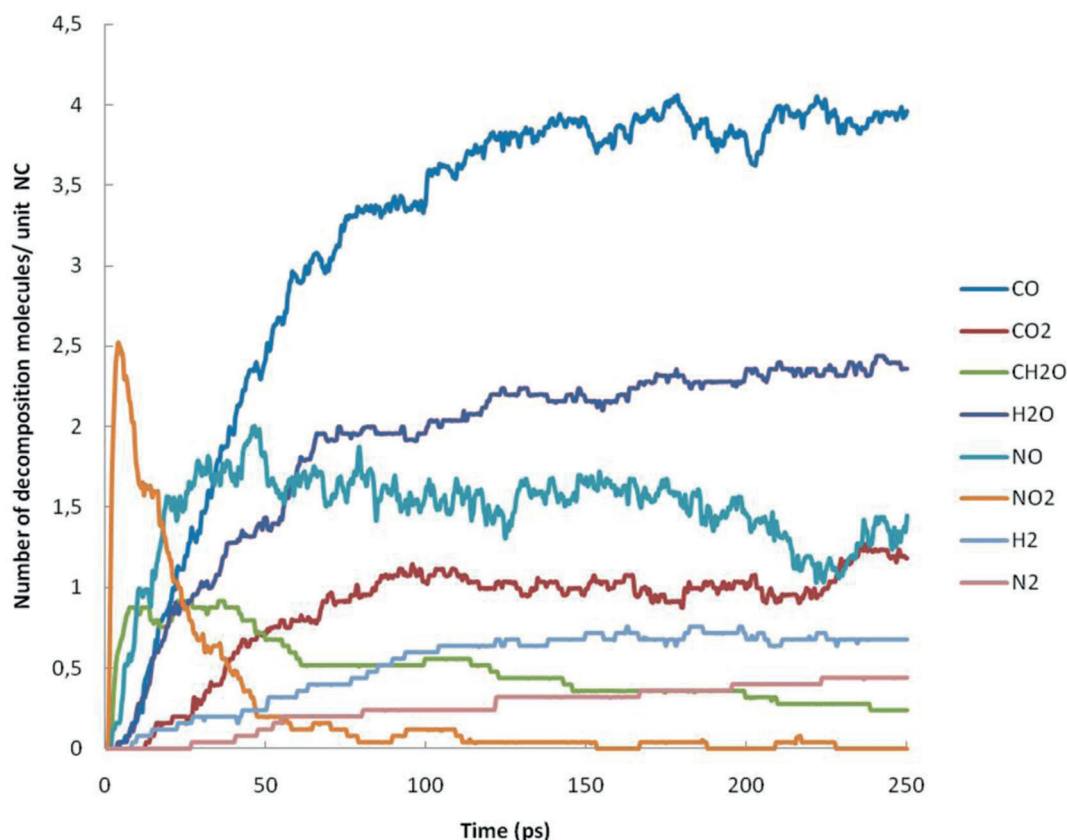


Figure 6. The number of decomposition molecules per NC unit. The density (292 kg m^{-3}) and temperature (3000 K) correspond to state 2. 25 NC units were used in the starting configuration of the simulation.

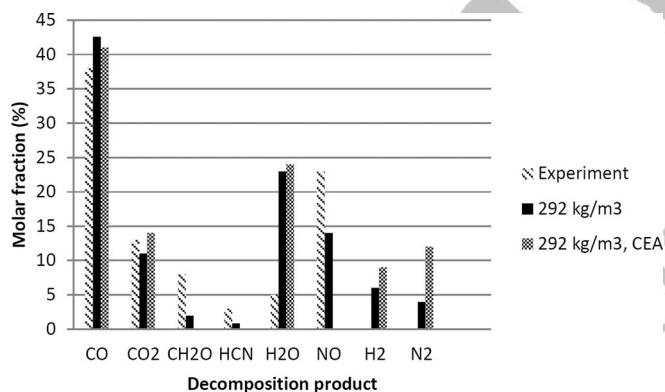


Figure 7. The molar fraction of decomposition products from NC. The density (292 kg m^{-3}) and temperature (3000 K) correspond to state 2. The same density and temperature are used in the thermodynamic equilibrium calculation. The experimental results are from Hiyoshi et al. [6].

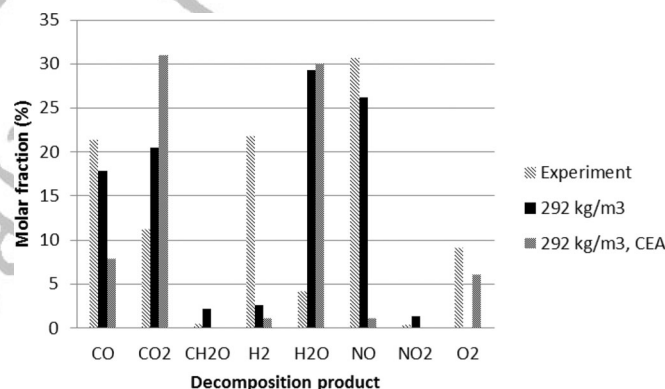


Figure 8. The molar fraction of decomposition products from NG. The density and temperature are 292 kg m^{-3} and 3000 K , respectively. The same density and temperature are used in the thermodynamic equilibrium calculation. The experimental results are from Roos et al. [7].

The formation of HCN by thermal decomposition of DPA is clearly dependent on the density in the first part of the decomposition process as shown in Figure 10. However, after 250 ps the number of HCN molecules is approximately at the same level for the different densities. Thermal de-

composition of EC shows dependency on temperature and density (Figure 11 and Figure 12). DPA generates around 0.3 molecules HCN per molecule DPA, and EC decomposition gives about 0.8 molecules HCN per molecule EC. Thus,

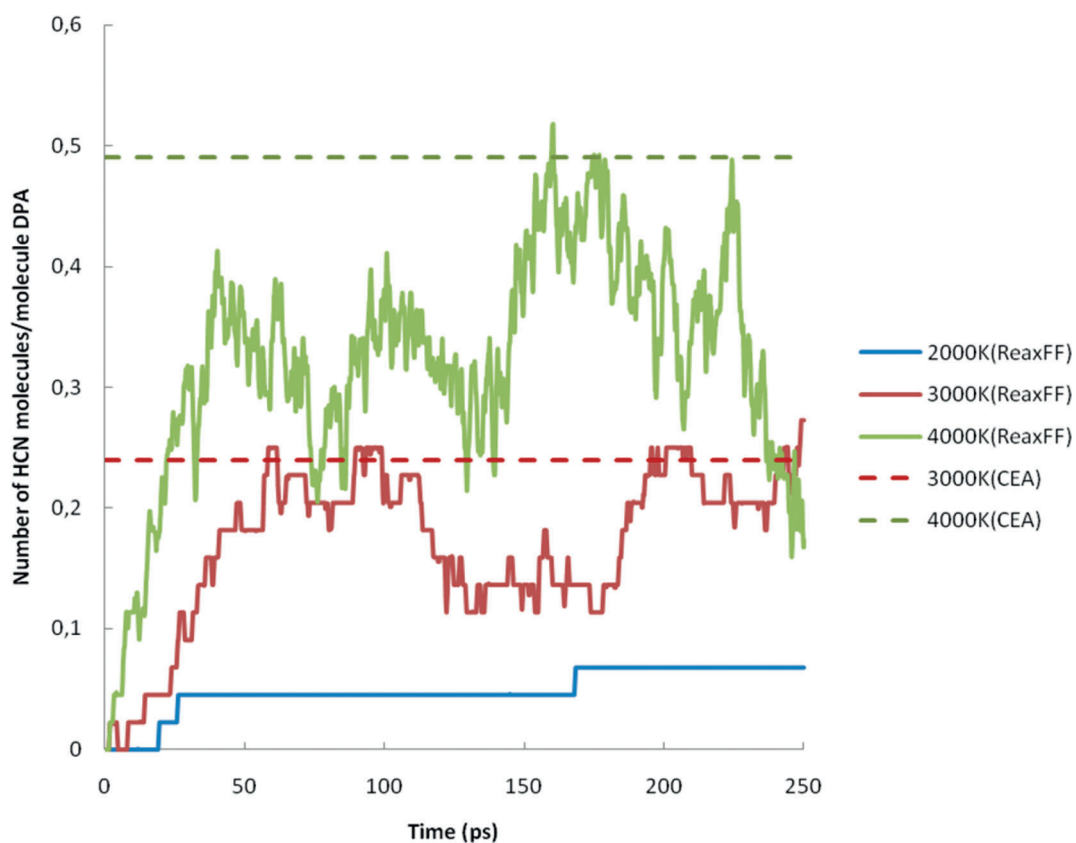


Figure 9. The number of HCN molecules per DPA molecule at various temperatures. The density is 292 kg m^{-3} . The dotted lines are thermodynamic equilibrium calculations.

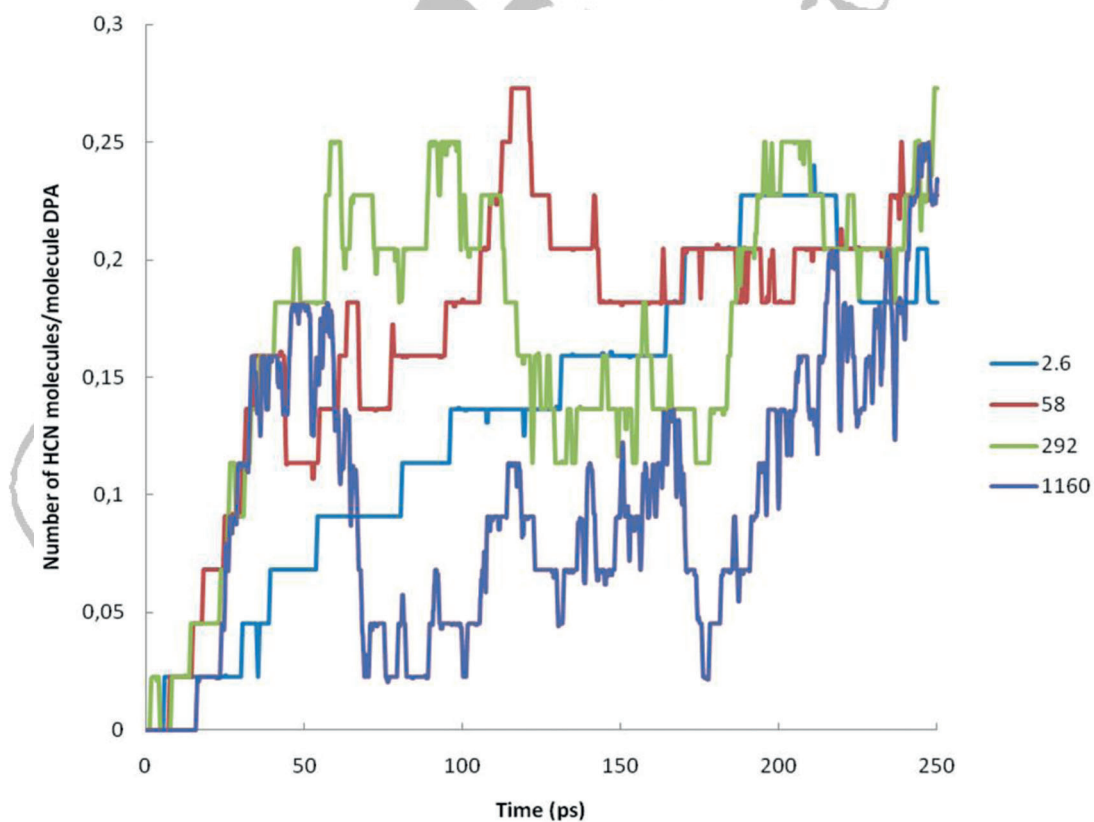


Figure 10. The number of HCN molecule per molecule DPA at various densities. The temperature is 3000 K.

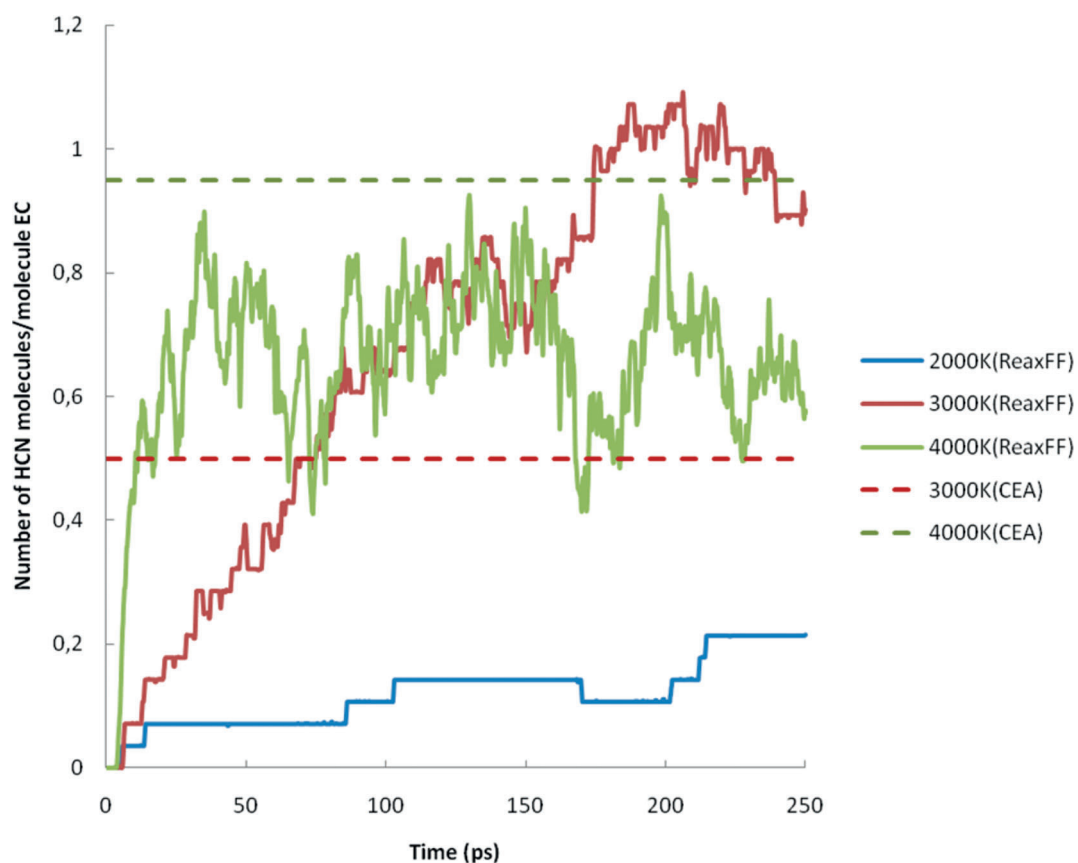


Figure 11. The number of HCN molecules per molecule EC at various temperatures. The density is 292 kg m^{-3} .

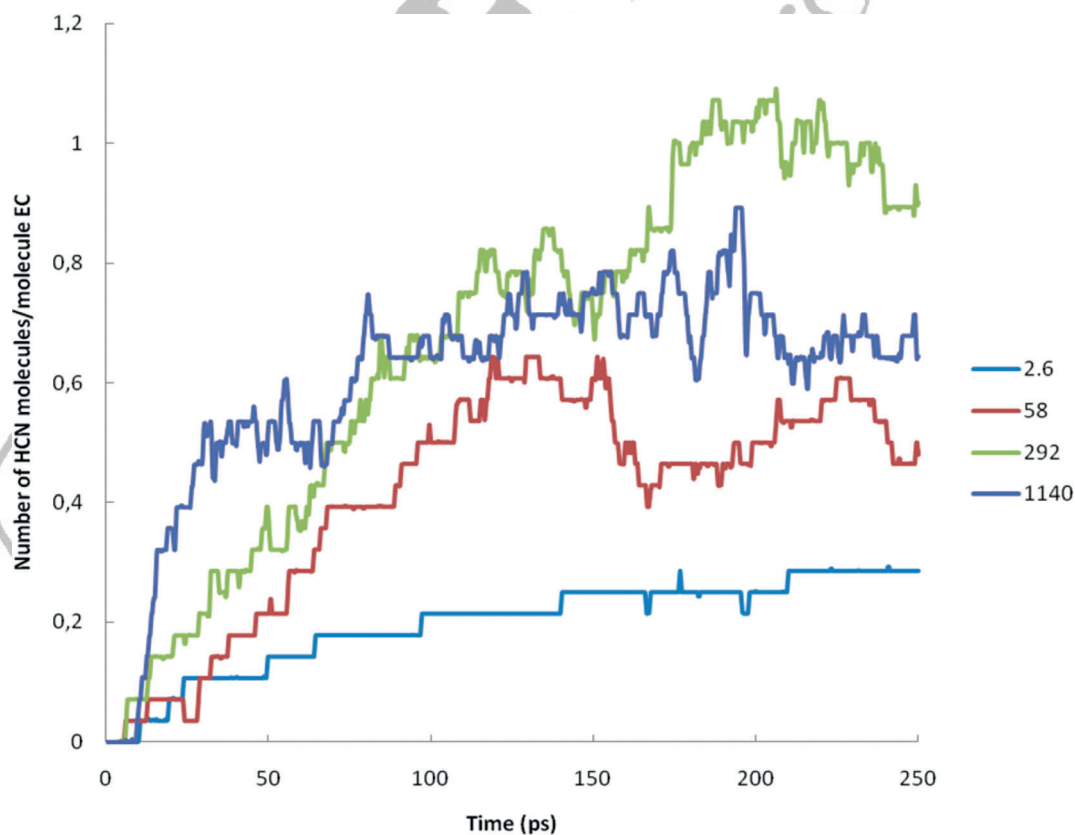


Figure 12. The number of HCN molecules per molecule EC at various densities. The temperature is 3000 K.

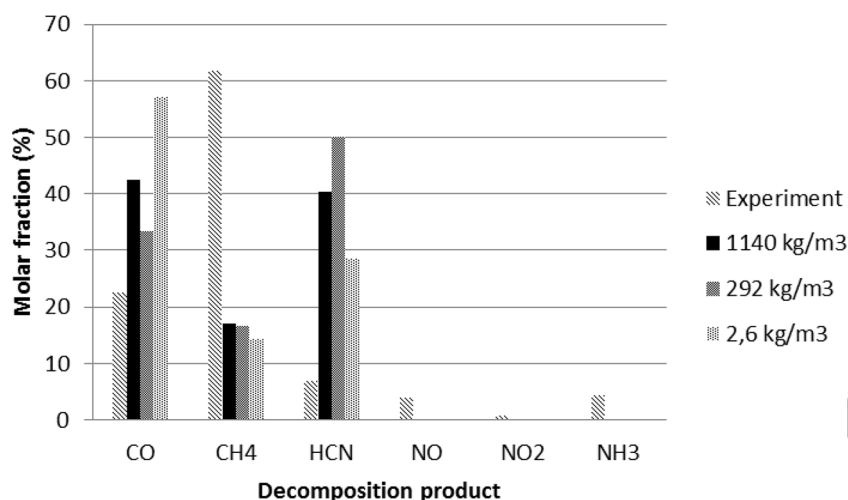


Figure 13. The molar fraction of decomposition products at various densities (2.6, 292 and 1140 kg/m³). The temperature was 3000 K.

these stabilizers can be a source for HCN in the combustion gas from gunpowder.

Moxnes et al. measured the amount of NH₃ from a rifle shot to be 11 mg per gram propellant [11]. Neither NC nor NG forms any NH₃ during the decomposition simulation in ReaxFF. On the other hand, NH₃ is formed as an intermediate during the decomposition simulation of EC. The maximum value of NH₃ in the simulation was one NH₃ molecule per five molecules EC. After 250 ps no NH₃ was present. De-

composition of DPA with ReaxFF-MD generated one NH₃ molecule per 50 molecules DPA after 250 ps.

We have performed pyrolysis experiments, where DPA and EC were thermally decomposed. DPA evaporated without any decomposition because no HCN or any other decomposition product was measured by FTIR. HCN and NH₃ are generated in the pyrolysis of EC. In Figure 13 the results for EC are compared with ReaxFF-MD simulations. We observed significant discrepancies between measurements

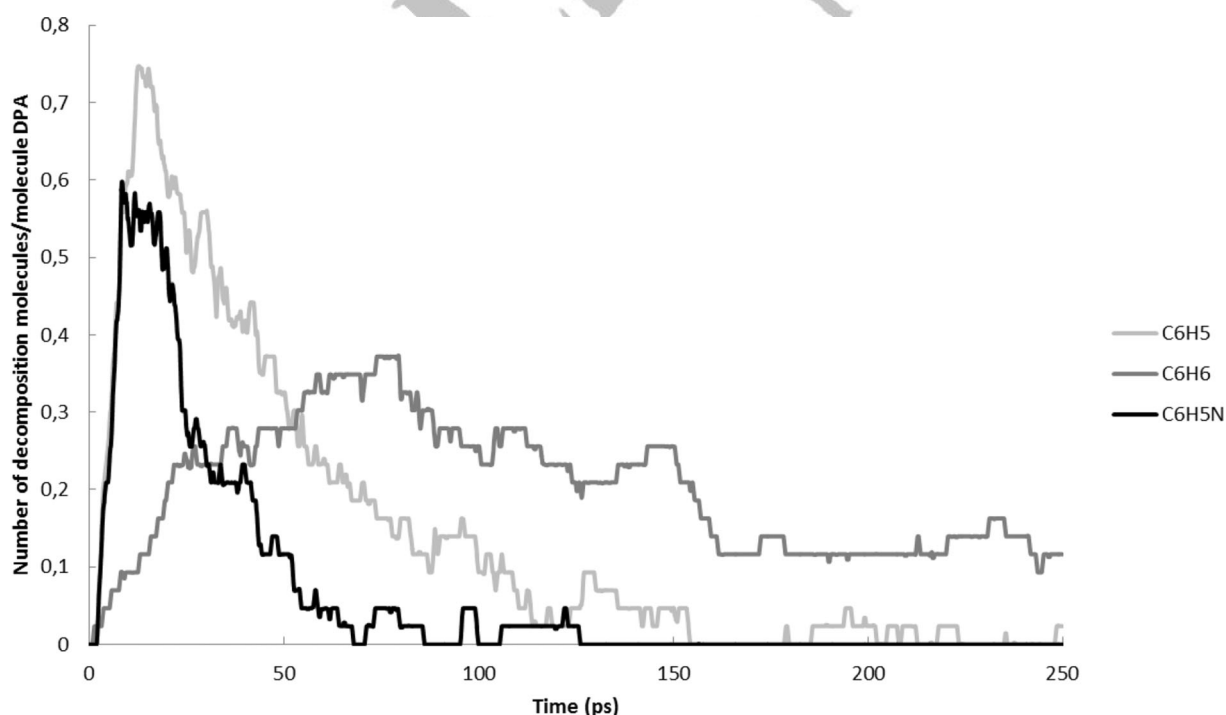


Figure 14. The number of aromatic decomposition molecules per molecule DPA. The temperature is 3000 K and the density is 292 kg m⁻³.

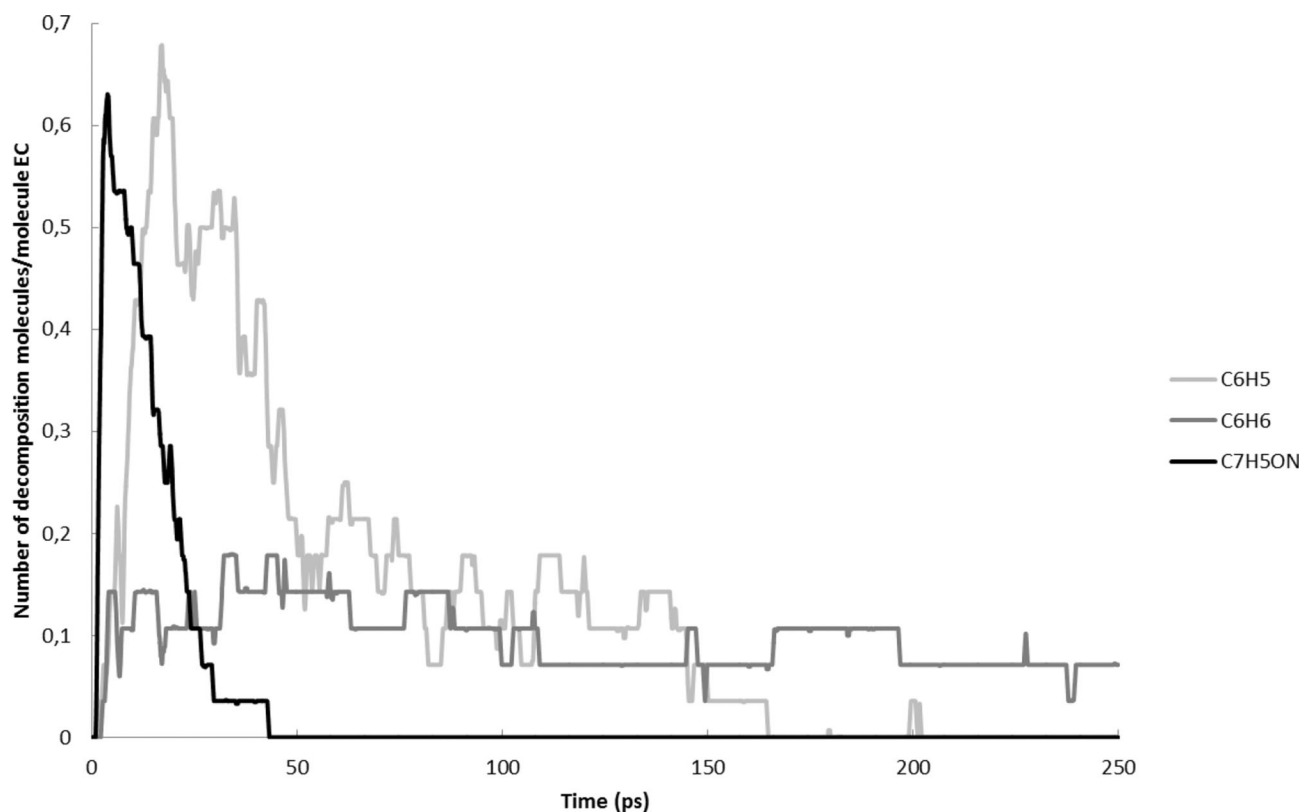


Figure 15. The number of aromatic decomposition molecules per molecule EC. The temperature is 3000 K and the density is 292 kg m^{-3} .

and simulations. This may be partly explained by vaporizing of EC. Furthermore, we measured more CH_4 than what simulated values predicted. The reason for this may be that aromatic decomposition products flowed down from the condenser and into the reagent bottle, which was heated by gas burners. This continued until the aromatic compounds were decomposed.

By simulating the thermal DPA decomposition, the main products are phenyl radical (C_6H_5), benzene (C_6H_6), and azanylbenzene ($\text{C}_6\text{H}_5\text{N}$), as shown in Figure 14. We also found a variety of aromatic species, but in minor amounts only. However, the simulations show that most of the aromatics degrade to hydrocarbon clusters, H_2 , HCN, amines, and small hydrocarbon species.

Ase et al. [1] measured the amount of benzene generated from a shot from an M16 rifle to be 0.17 mg per gram propellant. The propellant contained 0.75–1.5% DPA (and 3–6% dibutylphthalate), and the corresponding molar ratio benzene/DPA is therefore typically 1:25. This value is significantly lower than what is displayed in Figure 14. However, in order to compare the data from Ase et al. [1] with ReaxFF-MD results all the gunpowder ingredients have to be decomposed simultaneously.

EC decomposes thermally to phenyl radical (C_6H_5), benzene (C_6H_6), and isocyanatobenzene ($\text{C}_6\text{H}_5\text{NCO}$) and these

products are further broken down to hydrocarbon clusters, CH_4 , CO, HCN, H_2 and other small hydrocarbon molecules. Benzene is stable throughout the simulation time as seen in Figure 15.

4 Conclusions

Substance emissions produced by firing weapons with nitro-based propellants are in general highly complex mixtures of gases, vapors, and particulate substances. The measured HCN concentration from a gunshot is several orders of magnitude larger than any of their thermodynamically calculated concentrations anywhere in the gun barrel. By applying ReaxFF-MD calculations on nitrocellulose and the stabilizers in the gunpowder, we have found concentration levels in fair agreement with experimental results and to some extent consistent with thermodynamic calculations. We conclude that the concentrations of HCN are frozen in at high temperatures and not from the thermodynamic equilibrium conditions in the gunpowder gases. Thus, the concept of frozen non-equilibrium can be constructed. The stabilizers diphenylamine (DPA) and ethyl centralite (EC) seem to be essential for emission of HCN, NH_3 , and benzene.

Abbreviations

DPA – Diphenylamine (C₁₂H₁₁N)
 EC – Ethyl centralite (C₁₇H₂₀N₂O)
 HMX – Cyclotetramethylene tetranitramine (C₄H₈N₈O₈)
 NC – Nitrocellulose (C₆H₇N₃O₁₁)
 NG – Nitroglycerine (C₃H₅N₃O₉)
 PETN – Pentaerythritol tetranitrate (C₅H₈N₄O₁₂)
 RDX – Cyclotrimethylene trinitramine (C₃H₆N₆O₆)
 TATB – 1,3,5-Triamino-2,4,6-trinitrobenzene (C₆H₆N₆O₆)
 TATP – Triacetone triperoxide (C₉H₁₈O₆)

References

- [1] P. Ase, W. Eisenberg, S. Gordon, K. Taylor, A. Snelson, Propellant Combustion Product Analysis on an M16 Rifle and a 105 mm Caliber Gun, *J. Environ. Sci. Health A* **1985**, *20*, 337–368.
- [2] J. S. Felton, P. Lewis, M. G. Knize, G. Miller, *Mutagenicity of Burnt Gun Propellants in: Mutation and the Environment, Part E* (Eds.: M. L. Mendelsohn, R. J. Albertini), Wiley – Liss, New York **1990**, 243–249.
- [3] W. G. Palmer, A. W. Andrews, D. Mellini, J. A. Terra, F. J. Hoffmann, S. H. Hoke, Mutagenicity of Particulate Emission from the M16 Rifle: Variation with Particle Size, *J. Toxicol. Environ. Health* **1994**, *43*, 423–433.
- [4] L. Claxton, J. Huisingsh, Characterization of the Mutagens Associated with Diesel Particle Emissions, *Environ. Mutagen.* **1980**, *2*, 239.
- [5] F. Volk, H. Bathelt, Performance Parameters of Explosives: Equilibrium and Non-Equilibrium Reactions, *Propellants Explos. Pyrotech.* **2002**, *27*, 136–141.
- [6] R. I. Hiyoshi, T. B. Brill, Thermal Decomposition of Energetic Materials 83. Comparison of the Pyrolysis of Energetic Materials in Air vs. Argon, *Propellants Explos. Pyrotech.* **2002**, *27*, 23–30.
- [7] B. D. Roos, T. B. Brill, Thermal Decomposition of energetic Materials. Correlation of Gaseous Products with the Compositions of Aliphatic Nitrate Esters, *Combust. Flame* **2002**, *128*, 181–190.
- [8] D. M. Crokek, P. A. Kemme, J. M. Day, J. Cochran, Use of Pyrolysis GC/MS for Predicting Emission Byproducts from the Incineration of Double-Base Propellant, *Environ. Sci. Technol.* **2002**, *36*, 4346–4351.
- [9] J. C. Wakefield, *A Toxicological Review of the Products of Combustion*, Health Protection Agency, HPA-CHaPD-004, UK **2010**.
- [10] A. Snelson, P. Ase, K. Taylor, S. Gordon, *Combustion Product Evaluation of Various Charge Sizes and Propellant Formulations. Final Report*, U.S Army Medical Research and Development Command, Fort Detrick, Frederick, Maryland, 21702–5012. Contract no., DAMD17–88-C-8006 IIT Research Institute, Chicago, Illinois, 60616 (901019016), USA **1989**.
- [11] J. F. Moxnes, T. L. Jensen, E. Smestad, E. Unneberg, O. Dullum, Lead Free Ammunition Without Toxic Propellant Gases, *Propellants Explos. Pyrotech.* **2013**, *38*, 255–260.
- [12] E. J. Reed, J. D. Joannopoulos, L. E. Fried, Electronic Excitations in Shocked Nitromethane, *Phys. Rev. B* **2000**, *62*, 16500–16509.
- [13] M. R. Manaa, L. E. Fried, C. F. Melius, M. Elstner, T. Frauenheim, Decomposition of HMX at Extreme Conditions: A Molecular Dynamics Simulation, *J. Phys. Chem. A* **2002**, *106*, 9024–9029.
- [14] F. Shimojo, R. K. Kaila, A. Nakano, P. Vashishta, Embedded Divide-and-conquer Algorithm on Hierarchical Real-space Grids: Parallel Molecular Dynamics Simulation Based on Linear-scaling Density Functional Theory, *Comput. Phys. Commun.* **2005**, *167*, 151–164.
- [15] M. R. Manaa, E. J. Reed, L. E. Fried, N. Goldman, Nitrogen-rich Heterocycles as Reactivity Retardants in Shocked Insensitive Explosives, *J. Am. Chem. Soc.* **2009**, *131*, 5483–5487.
- [16] S. J. Stuart, A. B. Tutein, J. A. Harrison, A Reactive Potential for Hydrocarbons with Intermolecular Interactions, *J. Chem. Phys.* **2000**, *112*, 6472.
- [17] A. C. T. van Duin, S. Dasgupta, F. Lorant, W. A. Goddard III, ReaxFF: A Reactive Force Field for Hydrocarbons, *J. Phys. Chem. A* **2001**, *105*, 9396–9409.
- [18] A. C. T. van Duin, Y. Zeiri, F. Dubnikova, R. Kosloff, W. A. Goddard, Atomistic-scale Simulations of the Initial Chemical Events in the Thermal Initiation of Triacetone triperoxide, *J. Am. Chem. Soc.* **2005**, *127*, 11053–11062.
- [19] D. W. Brenner, O. A. Shenderova, J. A. Harrison, S. J. Stuart, B. Ni, S. B. Sinnott, Second Generation Reactive Empirical Bond Order (REBO) Potential Energy Expression for Hydrocarbons, *J. Phys. Condens. Matter* **2002**, *14*, 783–802.
- [20] A. Strachan, A. C. T. van Duin, D. Chakraborty, S. Dasgupta, W. A. Goddard, Shock Waves in High-energy Materials: The initial Chemical Events in Nitramine RDX, *Phys. Rev. Lett.* **2003**, *91*, 098301.
- [21] A. Strachan, E. M. Kober, Thermal Decomposition of RDX from Reactive Molecular Dynamics, *J. Chem. Phys.* **2005**, *122*, 054502.
- [22] L. Zhang, S. V. Zybin, A. C. T. van Duin, S. Dasgupta, W. A. Goddard, Carbon Cluster Formation during Thermal Decomposition of Octahydro-1,3,5,7-tetranitro-1,3,5,7-tetrazocine and 1,3,5-Triamino-2,4,6-trinitrobenzene high Explosives from ReaxFF Reactive Molecular Dynamics Simulations, *J. Phys. Chem. A* **2009**, *113*, 10619–10640.
- [23] T.-T. Zhou, F.-L. Huang, Effects of Defects on Thermal Decomposition of HMX via ReaxFF Molecular Dynamics Simulations, *J. Phys. Chem. B* **2011**, *115*, 278–287.
- [24] J. Tersoff, New Empirical Approach for the Structure and Energy of Covalent Systems, *Phys. Rev. B* **1988**, *37*, 6991–7000.
- [25] K. Nomura, R. K. Kaila, A. Nakano, P. Vashishta, A. C. T. van Duin, W. A. Goddard III, Dynamic Transition in the Structure of an Energetic Crystal during Chemical Reactions at Shock Front Prior to Detonation, *Phys. Rev. Lett.* **2007**, *99*, 148303.
- [26] J. Budzien, A. P. Thomsen, S. V. Zybin, Reactive Molecular Dynamics Simulations of Shock Through a Single Crystal of Pentaerythritol Tetranitrate, *J. Phys. Chem. B* **2009**, *113*, 13142–13151.
- [27] Z. Diao, Y. Zhao, B. Chen, C. Duan, S. Song, ReaxFF Reactive Force Field for Molecular Dynamics Simulations of Epoxy Resin Thermal Decomposition with Model Compound, *J. Anal. Appl. Pyrolysis* **2013**, *104*, 618–624.
- [28] Gaussian 09, Revision A.02, M. J. Frisch, G. W. Trucks, H. B. Schlegel, G. E. Scuseria, M. A. Robb, J. R. Cheeseman, G. Scalmani, V. Barone, B. Mennucci, G. A. Petersson, H. Nakatsuji, M. Caricato, X. Li, H. P. Hratchian, A. F. Izmaylov, J. Bloino, G. Zheng, J. L. Sonnenberg, M. Hada, M. Ehara, K. Toyota, R. Fukuda, J. Hasegawa, M. Ishida, T. Nakajima, Y. Honda, O. Kitao, H. Nakai, T. Vreven, J. A. Montgomery, J. E. Peralta, F. Ogliaro, M. Bearpark, J. J. Heyd, E. Brothers, K. N. Kudin, V. N. Staroverov, R. Kobayashi, J. Normand, K. Raghavachari, A. Rendell, J. C. Burant, S. S. Iyengar, J. Tomasi, M. Cossi, N. Rega, J. M. Millam, M. Klene, J. E. Knox, J. B. Cross, V. Bakken, C.

Adamo, J. Jaramillo, R. Gomperts, R. E. Stratmann, O. Yazyev, A. J. Austin, R. Cammi, C. Pomelli, J. W. Ochterski, R. L. Martin, K. Morokuma, V. G. Zakrzewski, G. A. Voth, P. Salvador, J. J. Dannenberg, S. Dapprich, A. D. Daniels, O. Farkas, J. B. Foresman, J. V. Ortiz, J. Cioslowski, D. J. Fox, Gaussian, Inc., Wallingford CT, **2009**.

[29] G. Sanford, B. J. McBride, Computer Program for Calculation of Complex Chemical Equilibrium Compositions and Applications I. Analysis, vol. 1331, NASA Reference Publication, **1994**.

[30] L. Martinez, R. Andrade, E. G. Birgin, J. M. Martinez, A Package for Building Initial Configurations for Molecular Dynamics Simulations, *J. Comput. Chem.* **2009**, *30*, 2157–2164.

Received: December 10, 2013

Revised: March 18, 2014

Published online: ■ ■ ■ ■, 0000

